Simplified Operational Guidance for Preventing Parametric Rolling*1

— Extension of Grim's Effective Wave Concept —

Naoya UMEDA*, Yuta UCHIDA**

1. INTRODUCTION

Since the case of the C11 class post-Panamax containership in head waves in 1998 [1], many accidents involving the loss of onboard containers due to the large heel of containerships in head, quartering and following waves have been reported [2]. Most large heels cannot be explained by a linear theory and are presumed to be due to parametric rolling. Parametric rolling typically means that only if the wave height exceeds a threshold, one roll cycle occurs during two encounter wave cycles, and the actual roll period is close to the natural roll period of the ship. In the C11 class containership accident, about 800 containers were lost or damaged due to a large heel of about 40°. Similar large parametric roll motions have also been observed in model experiments.

Although parametric rolling has been widely known in the theoretical research field [3], it was often regarded as a phenomenon that occurs in regular waves but may be unrealistic in irregular waves [4]. However, after Paulling et al. [5] observed parametric rolling of a free-running containership model in natural astern waves in San Francisco Bay in 1974 and Umeda et al. [6] realised parametric rolling of a free-running containership model in artificial short-crested irregular following waves in a model basin, parametric roll in following and quartering waves was recognised as a real threat to actual containerships at sea. Therefore, the International Maritime Organization (IMO) in 1995 [7] circulated operational guidance for following and quartering seas, which includes ship-independent guidance for parametric rolling focusing on the ratio of the encounter wave period to the ship's natural roll period. Later, partly as a result of a document from the United States [8] on the C11 class containership accident, the IMO in 2002 [9] started to develop means for preventing parametric rolling that also included head waves. Initially, the operational guidance in 1995 was expanded in a straightforward manner in 2007 to deal with parametric rolling in head waves [10]. In 2020, Interim Guidelines on the Second Generation Intact Stability Criteria including parametric rolling [11] were approved for trial use, and in 2022 the related Explanatory Notes [12] providing detailed calculation procedures were published. These new criteria, which are based on physics, deal not only with design but also with operational aspects, and provide simple two-level vulnerability criteria for ship design. If a ship under a certain condition fails to comply with them, its safety level may be demonstrated by probabilistic use of time-domain numerical simulation in short-crested irregular waves. Generally speaking, containerships and car carriers may often find it difficult to comply with these assessments because of their transom stern and exaggerated bow flare [13]. Thus, if the design measure is impractical, safe operation based on ship-dependent and physics-oriented operational guidance is required. For this purpose, full-probabilistic operational guidance and a simplified version can be utilised. The former is not always practical due to the high computational cost in terms of time. Although the example of the latter in the explanatory notes specifies only the ship speed, actual operation to avoid danger should also include the ship's course.

For practical use, operational guidance specifying not only the ship's speed but also its course is preferable. Therefore, this article attempts to provide a methodology to develop practical operational guidance for avoiding parametric rolling.

2. APPROACH ADOPTED FOR VULNERABILITY CRITERIA

The first level vulnerability criterion in the second generation intact stability criteria is the condition for the occurrence of parametric rolling regardless of the sea state. The second level consists of first and second checks: The former uses the weighted average of the occurrence conditions in typical sea states, while the latter uses the probability of sea states resulting in a parametric roll amplitude exceeding the critical magnitude. If any one of these three criteria is satisfied, the ship under the

---

*1 This article describes the details of the content read at the Spring Meeting of the Japan Society of Naval Architects and Ocean Engineers held in November 2022 [19].

* Professor emeritus, Osaka University

** Graduate School of Engineering, Osaka University

specified loading condition is judged as not vulnerable to parametric rolling. Among the three, only the second check of the second level vulnerability criteria can explicitly specify the critical heel angle, which depends on the lashing system, for example, the tier number of the lashing bridge. Since the second check of the second level vulnerability criteria seems most suitable for operational applications, this article will in principle attempt to adopt this methodology.

In this method, if a short-term sea state defined by the Bretschneider wave spectrum with the significant wave height and mean wave period is given, its spatial waveform is approximated by a regular wave using the Grim effective wave concept, and its 1/3 maximum largest amplitude is then used as the effective wave amplitude for estimating the GZ variation in a regular longitudinal wave. The parametric roll amplitude is determined by the encounter wave period depending on the ship speed and heading by numerically solving the uncoupled roll motion equation in the time domain. Here, the ship speed is set to the navigational speed, and the heading is uniformly distributed; that is, the effect of the wave heading on GZ variation is ignored as a conservative estimate. As a result, the encounter wave period can be calculated by changing the ship speed with the directional cosine of the wave heading. Finally, the probability of sea states with computed roll amplitudes larger than the critical heel angle is calculated by using the wave scatter diagram. If the obtained probability exceeds the acceptable value, the ship under the subject loading condition is judged vulnerable to parametric rolling failure.

3. SIMPLIFIED OPERATIONAL GUIDANCE IN THE IMO INTERIM GUIDELINES AS AN EXAMPLE

An example of the simplified operational guidance for parametric rolling is shown in paragraph 4.5.6.2.3 of the Interim Guidelines on the Second Generation Intact Stability Criteria. The parametric roll amplitude in longitudinal waves is calculated for the significant wave height, the zero-crossing mean wave period and the ship speed by using the method for the second check of the second level vulnerability criteria. If the amplitude is larger than 25°, the Guidelines request the ship master to avoid dangerous conditions defined by the significant wave height, the zero-crossing mean wave period and the ship speed, regardless of the wave heading. Although the ship speed is represented by “v_s” without definition in the Guidelines, judging from the text nearby, it could be read as the actual ship speed. If so, this guidance does not provide a dangerous ship course other than a dangerous ship speed.

On the other hand, section 4.5.6.2 of the IMO Interim Guidelines explicitly states that any guidance can be used if its required safety level is higher than that estimated by the full-probabilistic guidance using a numerical simulation in the time domain. Therefore, more advanced guidance specifying both the dangerous speed and course should be developed.

4. GENERALISATION OF THE GRIM EFFECTIVE WAVE CONCEPT

The second check of the second level vulnerability criteria utilises the Grim effective wave concept [14] to replace irregular waves with regular ones. Grim's paper only provides a formula for long-crested irregular longitudinal waves. However, the operational guidance is expected to be used for actual ship operational conditions, which means short-crested irregular waves with ship headings different from the main wave direction. Therefore, a formula for short-crested irregular quartering waves is derived here.

Normally, in a seakeeping theory, a ship response such as ship motions in irregular waves is handled stochastically under the assumption that the relationship between the incident wave and the ship response is linear. This means the spectrum of the ship responses in irregular waves can be estimated by the product of the incident wave spectrum and the response amplitude operator squared. Then, the significant amplitude of ship response is calculated by the Rayleigh distribution with the 0^{th} moment of the ship response spectrum. However, in the case of restoring variation due to waves, the relationship between incident waves and the restoring variation is nonlinear. In the example shown in Fig. 1 for a small trawler in regular waves whose length is equal to the ship length and crest or trough is located at the ship centre, the relationship between the incident wave amplitude and the wave-induced righting arm GZ at the heel angle of 10° has different slopes for the wave crest (negative value of the horizontal axis) and trough (positive value). Since the transom stern can be out of water when a wave trough is at the ship’s stern, the waterplane breadth at the stern can be zero. On the other hand, when a wave crest is at the ship's stern, the waterplane breadth at the stern can be slightly larger than the calm-water value. In addition, when the relative wave elevation exceeds the deck edge level, the waterplane breadth can change nonlinearly. As a result, the restoring variation due to waves differs from the basic assumption used in a seakeeping theory. On the other hand, the restoring variation can be evaluated even hydrostatically with the relative wave profile, and therefore can be regarded as nonlinear but without memory. The Grim effective wave concept utilises this fact.

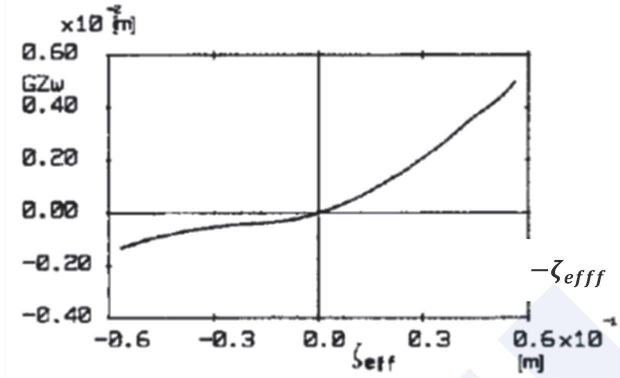

Fig. 1 GZ variation due to a regular wave whose length is equal to the ship's length and the crest or trough is located at the ship's centre for a small trawler at the heel angle of 10° [15)]

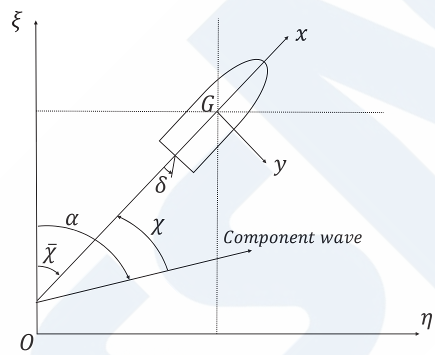

Fig. 2 Coordinate systems

As shown in Fig. 2, the space-fixed coordinate system O- ξ,η and the body-fixed coordinate system G- x,y are used. Here, the O-ξ axis indicates the main wave direction, α is the direction of a component wave, G is the centre of ship gravity (ξ_G, η_G) and $\bar{\chi}$ is the ship's heading from the main wave direction. Thus, the following relation exists.

$$\begin{aligned} \xi &= \xi_G + x cos\bar{\chi} - y sin\bar{\chi} \\ \eta &= \eta_G + x sin\bar{\chi} + y cos\bar{\chi} \end{aligned} \tag{1}$$

The wave elevation ζ_w as a function of position and time is represented as follows:

$$\begin{aligned} \zeta_w(\xi,\eta,t) &= \int_{-\frac{\pi}{2}}^{\frac{\pi}{2}} \int_0^\infty \sqrt{2S(\omega,\alpha)d\omega d\alpha}\, cos\left(\omega t - \frac{\omega^2}{g}\xi\, cos\,\alpha - \frac{\omega^2}{g}\eta\, sin\,\alpha + \psi\right) \\ &= \sum_{i=1}^{N} a_i cos\left[\omega_i t - \frac{\omega_i^2}{g}\{\xi cos\alpha_i + \eta sin\alpha_i\} + \psi_i\right] \\ &= \sum_{i=1}^{N} a_i cos\left[\omega_i t - \frac{\omega_i^2}{g}\{(\xi_G + x cos\bar{\chi} - y sin\bar{\chi})cos\alpha_i + (\eta_G + x sin\bar{\chi} + y cos\bar{\chi})sin\alpha_i\} + \psi_i\right] \end{aligned} \tag{2}$$

where t is a time, ψ is a random value between 0 and 2π, $S(\omega,\alpha)$ is the incident wave spectrum, and the component wave amplitude in discretisation is $a_i = \sqrt{2S(\omega,\alpha)d\omega d\alpha}$. $(i = 1, \cdots N)$

The effective wave is represented by Fig. 3 and Eq. (3).

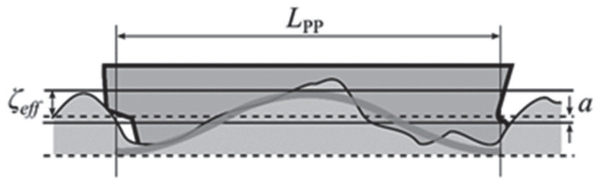

Fig. 3　Profile of the Grim effective wave

$$\hat{\zeta}_{eff}(x,t) = a(t) - \zeta_{eff}(t)\cos\frac{2\pi}{L}x \tag{3}$$

The effective wave can be determined by the least square method within the range of ship length -L/2<x<L/2 and its centre line y=0. Here, L indicates the ship length. Thus, the following value, J, should be minimised.

$$\begin{aligned}
\mathrm{J} &= \int_{-L/2}^{L/2}\left\{\zeta_w(\xi,\eta,t) - \hat{\zeta}_{eff}(x,t)\right\}^2 dx \\
&= \int_{-L/2}^{L/2}\left\{\sum_{i=1}^{N} a_i cos\left[\omega_i t - \frac{\omega_i^2}{g}\{(\xi_G + xcos\bar{\chi})cos\alpha_i + (\eta_G + xsin\bar{\chi})sin\alpha_i\} + \psi_i\right]\right. \\
&\qquad \left. - \left[a(\xi_G,\eta_G,\bar{\chi},t) - \zeta_{eff}(\xi_G,\eta_G,\bar{\chi},\ t)\cos\left(\frac{2\pi}{L}x\right)\right]\right\}^2 dx \\
&= \int_{-L/2}^{L/2}\left[\left\{\sum_{i=1}^{N} a_i cos\left[\omega_i t - \frac{\omega_i^2}{g}\{(\xi_G + xcos\bar{\chi})cos\alpha_i + (\eta_G + xsin\bar{\chi})sin\alpha_i\} + \psi_i\right]\right\}^2 - 2\left\{\sum_{i=1}^{N} a_i cos\left[\omega_i t\right.\right.\right. \\
&\qquad \left.\left. - \frac{\omega_i^2}{g}\{(\xi_G + xcos\bar{\chi})cos\alpha_i + (\eta_G + xsin\bar{\chi})sin\alpha_i\} + \psi_i\right]\right\}\left\{a(\xi_G,\eta_G,\bar{\chi},t)\right. \\
&\qquad \left. - \zeta_{eff}(\xi_G,\eta_G,\bar{\chi},\ t)\cos\left(\frac{2\pi}{L}x\right)\right\} - \{a(\xi_G,\eta_G,\bar{\chi},t)\}^2 \\
&\qquad \left. + 2\left\{a(\xi_G,\eta_G,\bar{\chi},t)\zeta_{eff}(\xi_G,\eta_G,\bar{\chi},\ t)\cos\left(\frac{2\pi}{L}x\right)\right\} - \left(\zeta_{eff}(\xi_G,\eta_G,\bar{\chi},\ t)\right)^2\cos^2\left(\frac{2\pi}{L}x\right)\right] dx
\end{aligned} \tag{4}$$

Therefore, the following formula should be satisfied.

$$\begin{aligned}
0 &= \frac{\partial J}{\partial \zeta_{eff}} \\
&= 2\int_{-L/2}^{L/2}\left\{\sum_{i=1}^{N} a_i cos\left[\omega_i t - \frac{\omega_i^2}{g}\left\{\left(\xi_G + xcos\bar{\chi}\right))cos\alpha_i + \left(\eta_G + xsin\bar{\chi}\right)sin\alpha_i\right\} + \psi_i\right]\right\}\cos\left(\frac{2\pi}{L}x\right) dx + \\
&\quad 2\left\{a\left(\xi_G,\eta_G,\bar{\chi},t\right)\int_{-\frac{L}{2}}^{\frac{L}{2}} cos\left(\frac{2\pi}{L}x\right)dx\right\} - 2\int_{-L/2}^{L/2}\zeta_{eff}\left(\xi_G,\eta_G,\bar{\chi},\ t\right)\cos^2\left(\frac{2\pi}{L}x\right) dx \\
&= 2\int_{-L/2}^{L/2}\left\{\sum_{i=1}^{N} a_i cos\left[\omega_i t - \frac{\omega_i^2}{g}\left\{\left(\xi_G\right)cos\alpha_i + \left(\eta_G\right)sin\alpha_i\right\}\right\} - \frac{\omega_i^2}{g}\left\{(xcos\bar{\chi})cos\alpha_i + (xsin\bar{\chi})sin\alpha_i\right\}\right\} + \\
&\quad \left.\left.\psi_i\right]\right\}\cos\left(\frac{2\pi}{L}x\right) dx - 2\int_{-L/2}^{L/2}\zeta_{eff}\left(\xi_G,\eta_G,\bar{\chi},\ t\right)\cos^2\left(\frac{2\pi}{L}x\right) dx
\end{aligned} \tag{5}$$

$$=2\int_{-L/2}^{L/2}\left\{\sum_{i=1}^{N} a_i cos\left[\omega_i t-\frac{\omega_i^2}{g}\{(\xi_G)cos\alpha_i+(\eta_G)sin\alpha_i\}-\frac{\omega_i^2}{g}xcos(\overline{\chi}-\alpha_i)+\psi_i\right]\right\} \cos\left(\frac{2\pi}{L}x\right) \ dx-\zeta_{eff}L$$

$$=2\int_{-L/2}^{L/2}\left\{\sum_{i=1}^{N} a_i cos\left[\omega_i t-\frac{\omega_i^2}{g}\{(\xi_G)cos\alpha_i+(\eta_G)sin\alpha_i\}+\psi_i\right]cos\left(-\frac{\omega_i^2}{g}xcos(\overline{\chi}-\alpha_i)\right)\right\} \cos\left(\frac{2\pi}{L}x\right) \ dx-\zeta_{eff}L$$

Using the following relation,

$$\int_{-L/2}^{L/2} cos\left(-\frac{\omega_i^2}{g}xcos(\bar{\chi}-\alpha_i)\right)\cos\left(\frac{2\pi}{L}x\right) \ dx$$
$$=\frac{1}{2}\int_{-L/2}^{L/2} cos\left(-\frac{\omega_i^2}{g}xcos(\bar{\chi}-\alpha_i)+\frac{2\pi}{L}x\right)+cos\left(-\frac{\omega_i^2}{g}xcos(\bar{\chi}-\alpha_i)-\frac{2\pi}{L}x\right) \ dx \qquad (6),$$
$$=\frac{-2\frac{\omega_i^2}{g}cos(\bar{\chi}-\alpha_i)sin\left(\frac{\omega_i^2 L}{2g}cos(\bar{\chi}-\alpha_i)\right)}{\left(\frac{\omega_i^2}{g}cos(\bar{\chi}-\alpha_i)\right)^2-\left(\frac{2\pi}{L}\right)^2}$$

the Grim effective wave ζ_{eff} is obtained as follows:

$$\zeta_{eff}(\xi_G,\eta_G,\bar{\chi},\ t;L)=\frac{4}{L}\sum_{i=1}^{N} a_i\frac{1}{\left(\frac{2\pi}{L}\right)^2-\left(\frac{\omega_i^2}{g}cos(\bar{\chi}-\alpha_i)\right)^2}$$
$$\cdot\left(\frac{\omega_i^2}{g}cos(\bar{\chi}-\alpha_i)\right) \ sin\left\{\frac{\omega_i^2}{2g}cos(\bar{\chi}-\alpha_i)\right\}$$
$$\cdot cos\left[\omega_i t-\frac{\omega_i^2}{g}\{\xi_G cos\alpha_i+\eta_G sin\alpha_i\}+\psi_i\right] \qquad (7)$$
$$=\sum_{i=1}^{N} a_i\frac{\left(\frac{\omega_i^2 L}{g}cos(\bar{\chi}-\alpha_i)\right)sin\left\{\frac{\omega_i^2 L}{2g}cos(\bar{\chi}-\alpha_i)\right\}}{\pi^2-\left(\frac{\omega_i^2 L}{2g}cos(\bar{\chi}-\alpha_i)\right)^2}$$
$$\cdot cos\left[\omega_i t-\frac{\omega_i^2}{g}\{\xi_G cos\alpha_i+\eta_G sin\alpha_i\}+\psi_i\right]$$
$$=\int_{-\frac{\pi}{2}}^{\frac{\pi}{2}}\int_{0}^{\infty}\sqrt{2S_{eff}(\omega,\alpha;L,\bar{\chi})d\omega d\alpha}\cdot cos\left[\omega t-\frac{\omega^2}{g}\xi_G\cos\alpha-\frac{\omega^2}{g}\eta_G\sin\alpha+\psi\right]$$

where

$$S_{eff}(\omega,\alpha;L,\bar{\chi}) = S(\omega,\alpha)\cdot\left[\frac{\left(\frac{\omega^2 L}{g}cos(\bar{\chi}-\alpha)\right)sin\left\{\frac{\omega^2 L}{2g}cos(\bar{\chi}-\alpha)\right\}}{\pi^2-\left(\frac{\omega^2 L}{2g}cos(\bar{\chi}-\alpha)\right)^2}\right]^2 \quad (8).$$

As shown above, the spectrum of the effective wave amplitude $S_{eff}(\omega,\alpha;L,\bar{\chi})$ can be calculated as a function of the frequency ω and the angle α when the ship length L and the wave heading $\bar{\chi}$ are given. When the denominator of Eq. (8) is zero, in other words, the length of the relevant component wave is equal to the ship's length, the spectrum density of the effective wave amplitude coincides with the spectrum density of the incident wave. Thus, this is consistent with the definition of the Grim effective wave. The specific density of the effective wave amplitude decreases when the wave heading increases from that of a pure following wave. When $\bar{\chi}-\alpha=\pi/2$, the spectrum density of the effective wave amplitude becomes zero. This formula coincides with that in Umeda & Yamakoshi [15].

Furthermore, by using the following formula,

$$\frac{\partial J}{\partial a}=0 \quad (9),$$

the mean value of the effective wave a can be obtained as follows:

$$a(\xi_G,\eta_G,\bar{\chi},\ t;L) = \int_{-\frac{\pi}{2}}^{\frac{\pi}{2}}\int_0^\infty \sqrt{2S_a(\omega,\alpha;L,\bar{\chi})d\omega d\alpha}\cdot cos\left[\omega t-\frac{\omega^2}{g}\xi_G\cos\alpha-\frac{\omega^2}{g}\eta_G\sin\alpha+\psi\right] \quad (10)$$

where its spectrum $S_a(\omega,\alpha;L,\bar{\chi})$ is given by

$$S_a(\omega,\alpha;L,\bar{\chi}) = S(\omega,\alpha)\cdot\left[\frac{sin\left\{\frac{\omega^2 L}{2g}cos(\bar{\chi}-\alpha)\right\}}{\frac{\omega^2 L}{2g}cos(\bar{\chi}-\alpha)}\right]^2 \quad (11).$$

When the denominator of Eq. (11) is zero, in other words, $\bar{\chi}-\alpha=\pi/2$, the spectrum density of the mean value of the effective wave becomes the spectrum density of incident waves.

5. ESTIMATION METHOD FOR RESTORING VARIATION USING THE GRIM EFFECTIVE WAVE CONCEPT

Once the Grim effective wave is given, the restoring variation due to waves can be estimated as follows. First, the righting arm in a regular longitudinal wave is calculated. Here, the wavelength is equal to the ship's length, and the wave crest or trough is situated at the ship's centre. The incident wave is assumed not to be disturbed by the ship, which is known as the Froude-Krylov assumption. Then, the incident wave pressure is integrated over the ship's submerged surface. Sinkage and trim should be iteratively determined with the ship's weight. The profile of an incident wave propagating in the direction of ξ, that is, ζ_w, and its pressure p are given by Eqs. (12) and (13), respectively.

$$\zeta_w(\xi,t)=\zeta_a cosk(\xi-ct) \quad (12)$$

$$p(\xi,\zeta,t)=\rho g\zeta-\rho g\zeta_a e^{-k\zeta}cosk(\xi-ct) \quad (13)$$

Here, the ζ-axis is pointed downward, ζ_a is the wave amplitude, k is the wave number and c is the wave celerity. Since the wave amplitude is not small in actual cases, the following practical formulae are often used.

$$p(\xi,\zeta,t) = \rho g\zeta - \rho g\zeta_a e^{-k\{\zeta-\zeta_w(\xi,t)\}} cos k(\xi - ct) \tag{14}$$

$$p(\xi,\zeta,t) = \rho g\zeta - \rho g\zeta_a e^{-kd} cos k(\xi - ct) \tag{15}$$

where d indicates the ship's mean draught. Further, the following expression can be obtained by expanding the exponential function into the Taylor expansion and ignoring higher-order terms.

$$p(\xi,\zeta,t) \approx \rho g\zeta - \rho g\zeta_a(1-kd) cos k(\xi - ct) \approx \rho g\{\zeta - \zeta_a cos k(\xi - ct)\} \tag{16}$$

In this case, the righting arm can be hydrostatically calculated with a sinusoidal wavy surface. Comparisons among the above formulae and a captive model experiment indicate that Eq. (16) is sufficient for practical purposes [16) 17)].

Repeating the above calculations for different wave amplitudes, GZ and GM can be obtained as functions of the effective wave amplitude so that they are represented as $GZ(\zeta_{eff})$ and $GM(\zeta_{eff})$, respectively. Thus, if the time series of ζ_{eff} is provided, the time series of $GZ(\zeta_{eff})$ and $GM(\zeta_{eff})$ can also be obtained. If the probability density function of the effective wave amplitude is given, stochastic representative values of the effective wave amplitude, such as the significant amplitude and the zero-crossing mean period, can be directly obtained by the transformation of random variables [18)].

Nevertheless, in the IMO Interim Guidelines on the Second Generation Intact Stability Criteria [11)], the 1/3 maximum amplitude of the effective wave amplitude is used for the input to the righting arm calculation in a regular wave for simplicity. More precisely, the 1/3 maximum amplitude obtained from the spectrum of the righting arm transformed from the effective wave amplitude with the narrow band assumption should be used as the amplitude of the effective wave for the righting arm calculation [18)]. Further, a probabilistic differential equation can be solved for the effective wave amplitude as a random process [19)].

6. ESTIMATION METHOD OF PARAMETRIC ROLL BY USING RESTORING VARIATION

Numerical simulation in the time domain is adopted in the IMO Interim Guidelines on the Second Generation Intact Stability Criteria [11)]. However, the obtained time series can exhibit roll motions other than the principal parametric roll assumed in the first level vulnerability criterion, such as chaos, as shown in the explanatory notes [12)]. Thus, expert knowledge may be required to handle the output properly. In addition, adding the direct roll excitation terms in the equation of motions in oblique waves may make the output even more complicated. Therefore, in this article, the averaging method is used to solve Eq. (17).

$$\ddot{\phi} + 2\alpha\dot{\phi} + \gamma\dot{\phi}^3 + {\omega_\phi}^2\phi + {\omega_\phi}^2 l_3\phi^3 + {\omega_\phi}^2 l_5\phi^5 + {\omega_\phi}^2(F + M\cos\omega_e t)\{\phi - (1/\pi^2)\phi^3\} = E\sin\omega_e t \tag{17}$$

where ϕ is the roll angle, α is the linear roll damping coefficient, γ is the cubic roll damping coefficient, ω_ϕ is the natural roll frequency, l_3 and l_5 are nonlinear restoring coefficients, F is the ratio of the mean value of GM variation to the calm-water GM and M is the ratio of the amplitude of GM variation to the calm-water GM. E represents the direct roll excitation moment with r as the effective wave coefficient, which can be calculated as follows:

$$E = \zeta_a r k {\omega_\phi}^2 sin\chi \tag{18}$$

The averaging method is applied to Eq. (17), assuming the following solution form.

$$\phi = A\cos\left(\frac{\omega_e}{2}t - \varepsilon_1\right) + B\sin(\omega_e t - \varepsilon_2) \tag{19}$$

where A, B, ε_1 and ε_2 are constants, the first term represents the subharmonic motion related to the parametric roll, and the second term indicates the harmonic motion related to the synchronous roll. The detailed formulae to be solved in order to determine A, B, ε_1 and ε_2 are provided by Sakai et al. [20]. It is noteworthy here that the averaging method without the direct excitation term [21) 22] is still useful because the second term is not particularly significant under conditions where parametric roll is important.

For the wave encounter frequency, which is the same as the frequency of restoring variation, the Interim Guidelines [11] use the linear wave dispersion of a regular wave whose length is equal to the ship length. Following the Grim effective wave concept, the wave encounter frequency should be estimated as the zero-crossing mean frequency of restoring variation estimated from the probability density function of restoring variation transformed from the Gaussian probability density function of the effective wave amplitude. However, according to a numerical study by Sakai et al. [23], the difference between the two methods seems small.

7. EXAMPLE OF APPLICATION OF SIMPLIFIED OPERATIONAL GUIDANCE

It appears to be possible to develop simplified operational guidance specifying the dangerous speed and course for a ship by following the methodology mentioned above and using the incident wave spectrum observed by onboard wave radar [24]. An example of the operational guidance prepared in this manner is shown in Figs. 4 and 5 as polar charts. Here, the averaging method with the direct excitation term is used as the solution method, and roll damping is estimated by using Ikeda's simplified method [25] with correction of its forward speed effect [26]. The subject ship is the C11 class containership, which has a natural roll period of 25.7 s. The assumed mean wave period, T01, is 12.5 s with the significant wave heights of 5 m and 7 m. The Bretschneider wave spectrum with a cosine squared directional distribution is used as the wave spectrum. The polar radius indicates the Froude number, and the polar angle shows the ship heading from the main wave direction. The region where the 1/3 maximum parametric roll amplitude exceeds 25° is shown in red as the dangerous zone.

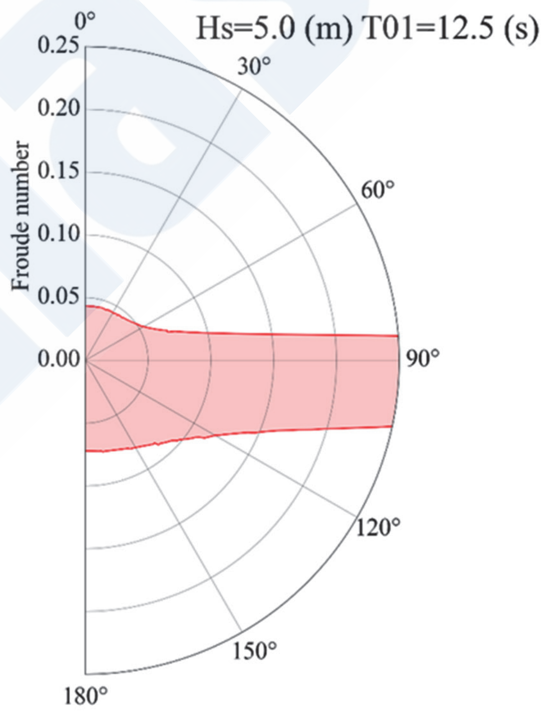

Fig. 4　Polar plot of simplified operational guidance for parametric rolling of the C11 class containership under a significant wave height of 5 m and mean wave period of 12.5 s

A dangerous zone exists in the operational condition where the encounter period is about half the ship's natural roll period. It exists at almost zero speed regardless of the heading angle, and extends to a higher speed region in beam waves. While the amplitude of the effective wave in regular beam waves is zero, short-crested irregular beam waves involve component waves encountering the ship with smaller heading angles, and thus are sufficient to cause a parametric roll.

When the significant wave height increases, the dangerous zone becomes somewhat broader. At the significant wave height of 5 m, an increase in the ship speed to a Froude number of 0.05 or higher in head waves effectively prevents parametric roll. At the significant wave height of 7 m, an increase to a Froude number of 0.07 or higher in head waves effectively prevents parametric roll.

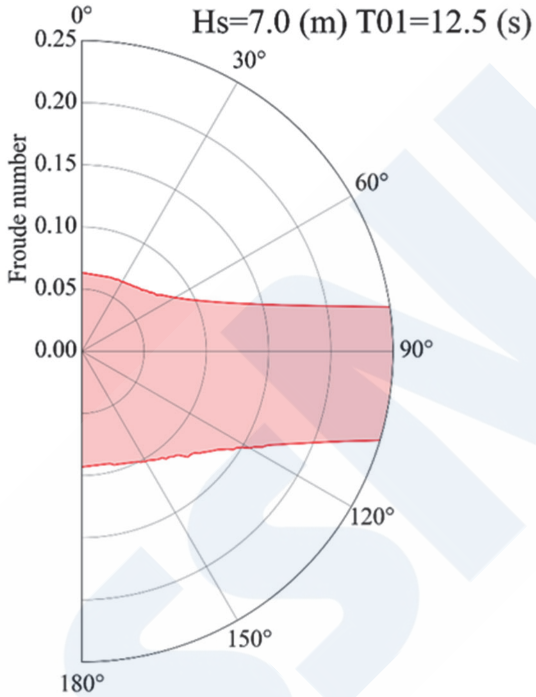

Fig. 5 Polar plot of simplified operational guidance for parametric rolling of the C11 class containership under a significant wave height of 7 m and mean wave period of 12.5 s

8. CONCLUSION

A method for developing simplified operational guidance for parametric rolling specifying the dangerous ship speed and dangerous course in short-crested irregular waves is proposed as an extension of the IMO vulnerability criteria using the generalised Grim effective wave concept. Examples of its application are provided as polar plots.

ACKNOWLEDGEMENTS

This study was partly carried out as a research activity of the Goal-based Stability Criteria Project of the Japan Ship Technology Research Association in fiscal year 2022 with funding by the Nippon Foundation.

REFERENCES

1) France, W. N., Levadou, M., Treakle, T.M., Paulling, J.R., Michel, R W.K and Moore, C., (2003): An Investigation of Head-Sea Parametric Rolling and its Influence on Container Lashing Systems, Marine Technology, 40(1), 1-19.
2) IMO (2023): Proposal for a new output on prevention of loss of containers at sea, submitted by Australia, Belgium, Chile, Denmark, France, Germany, Kingdom of the Netherlands, Morocco, Republic of Korea, Spain and IUMI, MSC 107/17/12.

3) Watanabe, Y. (1934): Dynamic Properties of the Transverse Instability of a Ship due to Pitching, Journal of Zosenkyokai, 53, 51-70, in Japanese.
4) Kerwin, J.E. (1955): Note on Rolling in Longitudinal Waves, International Shipbuilding Progress, 2(16), 597-614.
5) Oakley, O. H., Paulling, J. R., Wood, P. D. (1974): Ship Motions and Capsizing in Astern Seas, Proceedings of the 10th Symposium on Naval Hydrodynamics, 297-350.
6) Umeda, N., M. Hamamoto et al. (1995): Model Experiments of Ship Capsize in Astern Seas, Journal of the Society of Naval Architects of Japan, 177, 207-217.
7) IMO (1995): Guidance to the Master for Avoiding Dangerous Situations in Following and Quartering Seas, MSC/Circ. 707.
8) IMO (2002): Head-Sea Parametric Rolling and Its Influence on Container Lashing Systems, submitted by USA, SLF 45/6/7.
9) IMO (2002): Report to the Maritime Safety Committee, SLF 45/14, 20-25.
10) IMO (2007): Revised Guidance to the Master for Avoiding Dangerous Situations in Adverse Weather and Sea Conditions, MSC.1/Circ. 1228.
11) IMO (2020): Interim Guidelines on the Second Generation Intact Stability Criteria, MSC.1/Circ.1627.
12) IMO (2022): Explanatory Notes to Interim Guidelines on the Second Generation Intact Stability Criteria, MSC.1/Circ.1652.
13) IMO (2017): Selecting Calculation Methods and Standards for the Vulnerability Criteria for Parametric Roll, Pure Loss of Stability and Dead Ship Stability Failures Based on Sample Calculations, SDC 5/INF.4, Annex 17.
14) Grim, O. (1961): Beitrag zu dem Problem der Sicherheit des Schiffes im Seegang, Schiff und Hafen, 6, 490-497.
15) Umeda, N. and Yamakoshi, Y. (1994): Probability of Ship Capsizing due to Pure Loss of Stability in Quartering Seas, Naval Architecture and Ocean Engineering, 30, 73-85.
16) Umeda, N. (1985): Pure Loss of Stability in Following Waves, Journal of Fishing Boat Association, 258, 60-67.
17) Paulling, J.R. (1961): The Transverse Stability of a Ship in a Longitudinal Seaway, Journal of Ship Research, 4(4), 37-49.
18) Umeda, N. and Y. Yamakoshi (1986): Experimental Study on Pure Loss of Stability in Regular and Irregular Following Seas, Proceedings of the 3rd International Conference on Stability of Ships and Ocean Vehicles, Gdansk, 1, 93-99.
19) Umeda, N., Sakai, M. and Okamoto, H. (2022): Some Remarks on Simplified Operational Guidance for Parametric Rolling, Conference Proceedings of the Japan Society of Naval Architects and Ocean Engineers, 35, 437-440.
20) Sakai, M., Umeda, N., Yano, T., Maki, A., Yamashita, N., Matsuda, A., Terada, D. (2018): Averaging methods for estimating parametric roll in longitudinal and oblique waves, Journal of Marine Science and Technology, 23(3), 2, 413-424.
21) Umeda N., Hashimoto H., Vassalos D., Urano S., Okou K. (2004): Nonlinear dynamics on parametric roll resonance with realistic numerical modeling. International Shipbuilding Progress, 51(2/3), 205-220.
22) Maki, A., Umeda, N., Shiotani, S. and Kobayashi, E. (2011): Parametric rolling prediction in irregular seas using combination of deterministic ship dynamics and probabilistic wave theory, Journal of Marine Science and Technology, 16(3), 294-310.
23) Sakai, M., Umeda, N., Maki, A. (2019): Encounter frequency effect on the simplified design criteria against parametric roll, Ocean Engineering, 182, 21-27.
24) Yano, T., Umeda, N., Hirayama, K., Baba, M., Sakai, M. (2023): Wave Radar Application to the Simplified Parametric Roll Operational Guidance at Actual Sea. In Spyrou, K.J., Belenky, V.L., Katayama, T., Bačkalov, I., Francescutto, A. (eds.) Contemporary Ideas on Ship Stability. Fluid Mechanics and Its Applications, Vol. 134, Springer, Cham, 323-333.
25) Kawahara, Y., Maekawa, K., Ikeda, Y. (2011): A Simple Prediction Formula of Roll Damping of Conventional Cargo Ships on the Basis of Ikeda's Method and Its Limitation. In Almeida Santos Neves, M., Belenky, V., de Kat, J., Spyrou, K., Umeda, N. (eds.) Contemporary Ideas on Ship Stability and Capsizing in Waves, Fluid Mechanics and Its Applications, Vol. 97, Springer, Dordrecht, pp. 465-486.
26) Ikeda, Y. (2004): Prediction Methods of Roll Damping of Ships and Their Application to Determine Optimum Stabilisation Devices, Marine Technology, 41, 89-93.